Desalination and Water Treatment
www.deswater.com
doi: 10.1080/19443994.2015.1090919

57 (2016) 18202–18216
August

Taylor & Francis
Taylor & Francis Group

Anionic surfactant-modified rice straw for removal of methylene blue from aqueous solution

Azadeh Ebrahimian Pirbazari[a,b,*], Behnam Fakhari Kisom[a,b], Mohammad Ghamangiz Khararoodi[a,b]

[a]*Fouman Faculty of Engineering, College of Engineering, University of Tehran, P.O. Box 43515-1155, Fouman 43516-66456, Iran, Tel. +98 1327234927; Fax: +98 1327237228; emails: aebrahimian@ut.ac.ir (A. Ebrahimian Pirbazari), Behnam_fakhari@ut.ac.ir (B. Fakhari Kisom), M_ghamangiz@ut.ac.ir (M. Ghamangiz Khararoodi)*
[b]*Caspian Faculty of Engineering, College of Engineering, University of Tehran, P.O. Box 43841-119, Rezvanshahr 43861-56387, Iran*

Received 19 February 2015; Accepted 25 August 2015

ABSTRACT

This research reports on the development of organo-modified rice straw (RS) adsorbent prepared using sodium dodecyl sulfate (SDS) for removing methylene blue (MB), a model cationic dye, from aqueous solution. The natural and modified samples were characterized by scanning electron microscopy, nitrogen physisorption, and Fourier transform infrared spectroscopy. Batch adsorption experiments were carried out to remove MB from its aqueous solutions using SDS-modified RS (SMRS). The different parameters affecting the adsorption capacity such as pH of the solution, initial dye concentration, and contact time have been investigated. Analysis of adsorption results obtained at different temperatures showed that the adsorption pattern on the SMRS can be described perfectly with the Langmuir isotherm model compared with the Freundlich isotherm model, and the characteristic parameters for each adsorption isotherm were also determined, and the Langmuir adsorption capacity, Q_{max}, was found to be 296 mg/g for SMRS and 145 mg/g for RS at 303 K, respectively. The adsorption kinetic followed the pseudo-second-order kinetic model. Desorption studies suggest that MB adsorption onto the SMRS should be mainly controlled by the hydrophobic interaction mechanism, along with a considerable contribution of the cationic exchange mechanism.

Keywords: Rice straw; Sodium dodecyle sulfate; Methylene blue; Adsorption; Isotherm; Kinetic; Mechanism

1. Introduction

Adsorption technique is quite popular due to its simplicity as well as the availability of a wide range of adsorbents, and it is proved to be an effective and attractive process for the removal of refractory pollutants (including dyes and heavy metal ions) from wastewater [1–3]. Use of activated carbon as adsorbent has been found to be effective, but it is too expensive and the spent activated carbon can be regenerated with some mass lost. Thus, there is a demand for other adsorbents, such as inexpensive material from agricultural byproducts and industry waste with simple pretreatment step [3]. Some of the advantages of using agricultural waste for wastewater treatment

---

*Corresponding author.

include simple technique, requires little processing, good adsorption capacity, selective of adsorption effluent, low cost, free availability, and easy regeneration [2]. Besides, the exhausted adsorbents can be disposed of by burning and the heat is used for steam generation [4]. However, the application of untreated agricultural or plant waste as adsorbents can also bring several problems such as low adsorption capacity, high chemical oxygen demand (COD), and biological oxygen demand (BOD) as well as total organic carbon (TOC) due to the release of soluble organic compounds contained in the plant wastes [5]. Recently, comparative studies of cationic and anionic dye adsorption by agricultural solid wastes and some other low-cost adsorbents were reported [2,6–8]. Therefore, the agricultural wastes need to be treated or modified before being used as adsorbent. Rice straw (RS) is a lignocellulosic agricultural byproduct containing cellulose (37.4%), hemicellulose (44.9%), lignin (4.9%), and silicon ash (13.1%). The disposal of RS by open-field burning frequently causes serious air pollution, hence, new economical technologies for RS disposal and utilization must be developed. Many ideas have been suggested for valorizing RS as pulp and paper, construction materials, compost fuel, and production of chemicals such as ethanol, bio-adsorbents, and precursors for activated carbons [9].

In recent years, the use of surfactants in water and wastewater treatment has been specifically preferred to separation of metal ions and other toxic substances [10–15]. Surfactant molecules are composed of both hydrophilic and hydrophobic moieties and extensively used in various industrial processes such as textiles, pulp, and paper industry as well as our daily life. Surfactant–dye associations are important in various dyeing processes such as textiles dyeing, photography, and pharmaceuticals processes [16]. Surfactants play a useful role in the textile-dying processes due to their general action as leveling, dispersing, and wetting agents. Therefore, surfactants are considered as ideal and suitable components in the textile processing which requires liquid that quickly and uniformly wets the fiber surface. The surfactants act mostly in two ways, either by the formation of a complex species with ionic dyes or adsorption into the fiber [17]. Methylene blue (MB) is the most commonly used substance for dying cotton, wood and silk. It can cause eye burns which may be responsible for permanent injury to the eyes of human and animals. Although MB is seen in some medical uses in large quantities, it can also be widely used in coloring paper, dyeing cottons, wools, coating for paper stocks, etc. Though MB is not strongly hazardous, it can cause some harmful effects. Acute exposure to MB will cause increased heart rate, vomiting, shock, Heinz body formation, cyanosis, jaundice, and quadriplegia and tissue necrosis in humans [18].

To the best of our knowledge, the application of SDS-modified RS for MB removal from aqueous environment has not been reported so far. The aim of this work is to present and investigate an efficient methodology for color treatment of industrial wastewater effluent using a chemically designed and modified adsorbent based on RS-immobilized anionic surfactant, SDS, for the adsorptive removal of MB as an example of cationic dyes. Optimization of all experimental controlling factors and conditions such as reaction contact time, pH, adsorbent dosage, and initial dye concentration as well as mechanism of adsorption were also explored and evaluated.

2. Experimental

2.1. Materials

The RS used in this study was obtained from a local rice field of Rasht in Iran. The collected materials were washed several times with boiled water and finally with distilled water to remove any adhering dirt. The washed materials were then dried in the oven at 60˚C for 48 h. The dried RS was then ground and sieved into a size range of 100–500 μm. Finally, the resulting product was stored in airtight container for further use. The MB purchased from Merck (No. 115943), was selected as presentative reactive dye for this study. A stock solution of MB was prepared by dissolving 1.0 g of MB in 1 L of deionized water, and the concentrations of MB used (50–500 mg/L) were obtained by dilution of the stock solution. The pH of the solution was adjusted to the desired value by adding a small quantity of 0.01 M HCl or 0.01 M NaOH. SDS solutions were prepared from commercially available product (Merck, 8.22050) dissolved in distilled water.

2.2. Modification of RS by SDS and characterization

The solution of SDS was prepared below its critical micellar concentration (CMC = 0.0082 M), as beyond CMC, the surface modification was not effective. 100 mL of 2×10^{-3} M SDS solution was treated with 10.0 g of RS and shaken in a temperature-controlled shaker at 180 rpm for 3 h at 303 K. The SDS-modified RS (SMRS) was then filtered and washed with deionized water till conductance of filtrate was less than 0.05 μS. The SMRS was then dried in hot air oven at 80˚C for 24 h. This was then stored in airtight container for further use.

Fourier transform infrared (FTIR) analysis was applied to determine the surface functional groups, using FTIR spectroscope (FTIR-2000, Bruker), where the spectra were recorded from 4,000 to 400 cm^{-1}. Surface morphology was studied using scanning electron microscopy (Vegall-Tescan Company). Specific surface area based on nitrogen physisorption was measured by Sibata surface area apparatus 1100. The samples were degassed at 100˚C for 2 h prior to the sorption measurement.

2.2.1. *pH$_{pzc}$ calculation method*

In pH$_{\text{pzc}}$ determination, 0.01 M NaCl was prepared and its pH was adjusted in the range of 2.0–11.0 by adding 0.01 M NaOH or HCl. Then, 50 mL of 0.01 M NaCl each was put in conical flask and then 0.1 g of SMRS was added to these solutions. These flasks were kept for 72 h and final pH of the solution was measured using pH meter. Graphs were then plotted for pH$_{\text{final}}$ vs. pH$_{\text{initial}}$.

2.3. *Adsorption procedure*

Equilibrium isotherms were determined by shaking a fixed mass of SMRS (0.2 g) with 100 mL of MB solutions with different initial concentrations (in the range of 50–500 mg/L) in 250-mL glass Erlenmeyer's flasks at a temperature of 30˚C and pH 7.0. The procedure was repeated for temperatures 40 and 50˚C. Initial pH adjustments were carried out by adding either 0.01 M hydrochloric acid or 0.01 M sodium hydroxide solution. After shaking the flasks at 180 rpm for 2 h, the reaction mixtures were filtered through filter paper, and then the filtrates was analyzed for the remaining MB concentrations with spectrometry at the wavelength of maximum absorbance, 664 nm, using a double-beam UV–Vis spectrophotometer (Shimadzu, Model UV2100, Japan).

2.4. *Kinetic studies*

Adsorption kinetics experiments were performed by contacting 200 mL of MB solution of different initial concentrations ranging from 50 to 200 mg/L with 0.4 g of SMRS in a 500-mL stopper red conical flask at room temperature. At fixed time intervals, the samples were taken from the solution and were analyzed.

2.5. *Isotherm modeling*

The nonlinear forms of the Langmuir and Freundlich isotherm models were used to analyze the equilibrium isotherm data [19]. The fitness of these models was evaluated by the nonlinear coefficients of determination (R^2). The Matlab (version 7.3) software package was used for the computing. The Langmuir adsorption isotherm assumes that adsorption takes place at specific homogeneous sites within the adsorbent and has found successful application for many processes of monolayer adsorption. The Langmuir isotherm can be written in the form:

$$q_e = (Q_{\max} K_L C_e)/(1 + K_L C_e) \tag{1}$$

where q_e is the adsorbed amount of the dye, C_e is the equilibrium concentration of the dye in solution, $Q_{\max}$ is the monolayer adsorption capacity, and K_L is the Langmuir adsorption constant. The Freundlich isotherm is an empirical equation which assumes that the adsorption occurs on heterogeneous surfaces. The Freundlich equation can be expressed as follows:

$$q_e = K_F C_e^{1/n} \tag{2}$$

where K_F and $1/n$ are the fitting constants which can be regarded roughly, the capacity and strength of adsorption, respectively.

2.6. *Kinetic models*

The Lagergren rate equation [20] is one of the most widely used adsorption rate equations for the adsorption of solute from a liquid solution. The pseudo-first-order kinetic model of Lagergren may be represented by:

$$\frac{dq}{q_e} - q = k_1 dt \tag{3}$$

Integrating this equation for the boundary conditions $t = 0$ to $t = t$ and $q = 0$ to $q = q_t$, gives:

$$\ln(q_e - q_t) = \ln q_e - k_1 t \tag{4}$$

where q_e and q_t are the amounts of adsorbate (mg/g) at equilibrium and at time t (min), respectively, and k_1 is the rate constant of pseudo-first-order adsorption (min^{-1}). The validity of the model can be checked by linearized plot of $\ln(q_e - q_t)$ vs. t. Also, the rate constant of pseudo-first-order adsorption is determined from the slope of the plot.

The pseudo-second-order equation based on adsorption equilibrium capacity can be expressed as follows:

$$dq/(q_e - q_t)^2 = k_2 dt \tag{5}$$

Taking into account, the boundary conditions $t = 0$ to $t = t$ and $q = 0$ to $q = q_t$, the integrated linear form the above equation can be rearranged to the following equation:

$$1/(q_e - q_t) - 1/q_e = k_2 t \tag{6}$$

Rearranging the variables gives the following equation:

$$t/q_t = 1/k_2 q_e^2 + t/q_e \tag{7}$$

where the theoretical equilibrium adsorption capacity (q_e) and the second-order constants k_2 (g/mg min^{-1}) can be determined experimentally from the slope and intercept of plot t/q_t vs. t.

2.7. Statistical analysis

All experiments were performed in duplicate and the mean values were presented. The data were analyzed by a one-way analysis of variance (ANOVA) using SPSS11.5 for Windows. The data were considered statistically different from control at $p < 0.05$.

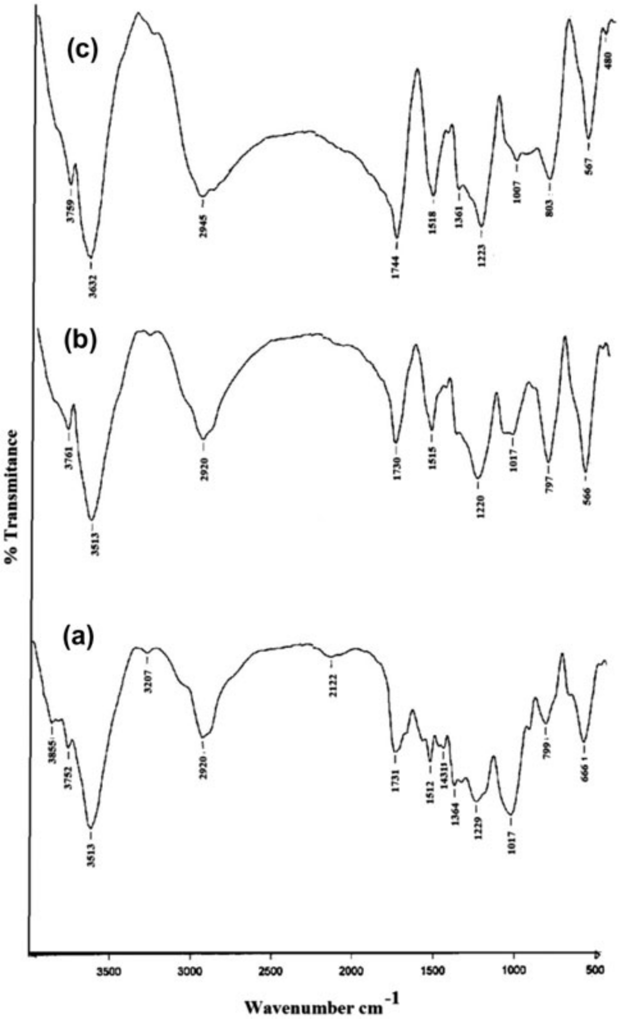

Fig. 1. FTIR spectra of (a) RS, (b) SMRS, and (c) SMRS after MB adsorption.

3. Result and discussion

3.1. FTIR spectral analysis

A closer insight into the biomass surface properties was obtained by comparing the FTIR spectra of prepared samples (Fig. 1) in the range of 400–4,000 cm^{-1}. The RS is constituted basically by cellulose, hemicellulose, lignin, extractives, water, and mineral ash which is in large amount, SiO_2. The lignin is promptly available to interact with cations, firstly by exchanging with protons and subsequently by chelating with the cations [21]. FTIR spectra of RS, SMRS, and SMRS after MB adsorption are shown in Fig. 1. In FTIR spectrum of RS (Fig. 1(a)), the broad absorption peak around 3,518 cm^{-1} is attributed to the stretching of H-bonded hydroxyl groups. The other adsorption at 2,920 cm^{-1} relates to the C–H stretching. The peak observed at 797 cm^{-1} in raw RS corresponds to the glycoside linkages deforming with ring vibration and OH bending [22]. The absorption bands at 1,800–1,300 cm^{-1} are the characteristics of C=C in aromatics ring [23].

The absorption bands at 1,017 and 666 cm^{-1} could be attributed to Si–O stretching and Si–O bending, indicating the presence of silica [21]. FTIR spectrum of the SMRS (Fig. 1(b)) shows more intense vibrations compared to RS at 3,513 and 2,920 cm^{-1} assigned to the $-CH_2$ group from SDS and the peak observed at 1,220 cm^{-1} could be assigned to $-SO_3$ stretching vibration [24], and these suggest that the SDS have been successfully modified the surface of RS. However, the FTIR spectra of SMRS and SMRS after MB adsorption were found to exhibit similar functional groups due to the domination of the functional groups of RS in this sorbent as the major component in these materials.

3.2. SEM and nitrogen physisorption analysis

Fig. 2 shows the scanning electron microscope (SEM) images of RS, SMRS, and SMRS after MB adsorption with two magnifications. It is evident from the obtained SEM images that surfactant modification is significantly responsible to alter the physicochemical properties of the materials. From the surface of RS (Fig. 2(a)), a large number of heterogeneous pores and aggregate particles can be observed. The pores may be originated from intercellular gaps [25], and the particles observed on RS possibly are silica residues [26]. Cao et al. [27] determined the component of these aggregate particles by energy-dispersive X-ray spectroscopy (EDX) contains O 64.79%, C 20.21%, Si 7.72%, K 5.22%, P 0.9%, Cl 0.89%, and Mg 0.59%. This suggests these silicon-containing materials may be

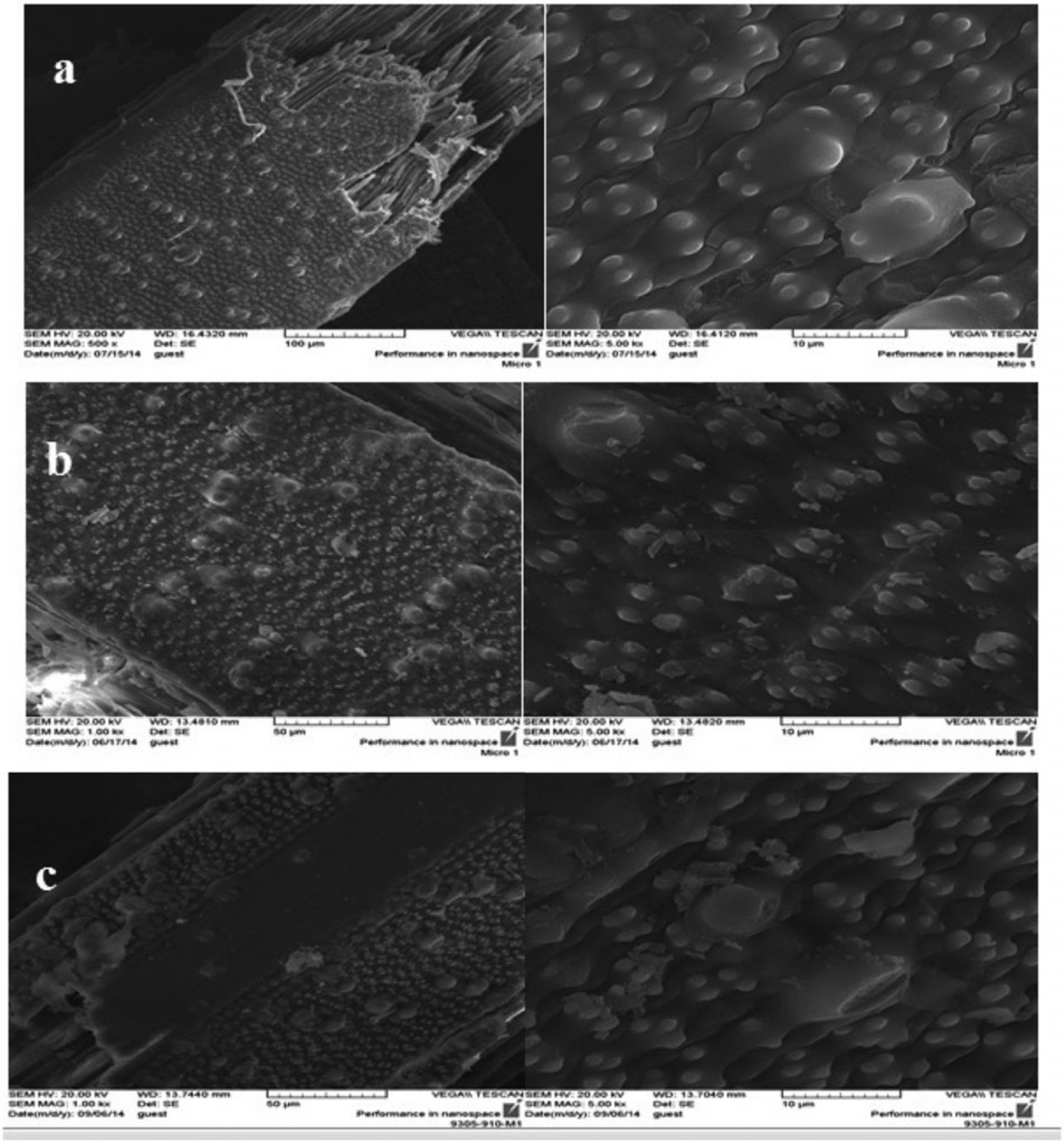

Fig. 2. SEM images of (a) RS, (b) SMRS, and (c) SMRS after MB adsorption.

related to the earth in which the rice was planted. After modification by SDS, a significant change was observed in surface morphology of the RS (Fig. 2(b)). The SMRS appears to possess more homogenous surfaces and well-organized porous structure than the RS (Fig. 2(b)). The surface of SMRS after MB adsorption (Fig. 2(c)), however, shows that the pores of RS are covered with MB molecules.

The specific surface area of RS and SMRS based on nitrogen physisorption were determined by the Brunauer–Emmett–Teller (BET) theory. It was found that the surface area of RS and SMRS were 58 and 150 $m^2 g^{-1}$, respectively. As Nadeem et al. reported [28], anionic (SDS) and cationic (CTAB) surfactant enhanced the characteristics of adsorbent better than the nonionic one (Triton X-100). The enhancement can be attributed to the typical properties of micelle formation, adsorption, wetting ,and solubilization. Being amphipathic in nature, surfactant-modified surfaces can offer enhanced surface area and wetting (water or oil wet) according to the requirement because surfactant molecules are capable of organizing themselves accordingly. Moreover, the presence of electrostatic interactions facilitates the possibility for selective adsorption as well. In mechanism section, we will give details about the role of surfactant in MB adsorption.

3.3. *Effect of initial concentration and contact time on MB adsorption*

The percentage of dye removal is highly dependent on the initial amount of dye concentration. The effect of the initial dye concentration factor depends on the immediate relation between the dye concentration and the available binding sites on an adsorbent surface. Generally, the percentage of dye removal decreases with an increase in initial dye concentration, which may be due to the saturation of adsorption sites on the adsorbent surface [8] and the adsorption capacity increased with an increase in the initial concentration of the dye. At low concentrations, there will be unoccupied active sites on the adsorbent surface, and when the initial dye concentration increases, the active sites required for adsorption of the dye molecules will not be available [29]. However, the increase in the initial dye concentration caused an increase in the loading capacity of the adsorbent and this may be due to the high driving force for mass at a high initial dye concentration [30]. In other words, the residual concentration of dye molecules will be higher for higher initial dye concentrations. In the case of lower concentrations, the ratio of the initial number of dye molecules to the available adsorption sites is low and subsequently the fractional adsorption becomes independent of the initial concentration.

Fig. 3 shows the effect of the initial dye concentration (50–200 mg/L) on the adsorption of MB. It was observed that amount of MB adsorbed was rapid for the first 20 min and thereafter it proceeded at a slower rate (20–60 min) and finally reached saturation. The equilibrium adsorption increases from 7.29 to 34.50 mg/g, with increase in the initial MB concentration from 50 to 200 mg/L. The findings are because as the initial concentration increases, the mass transfer driving force becomes larger, hence resulting in higher MB adsorption [31]. It is also shown in Fig. 3 that the contact time needed for MB solutions with initial concentrations of 50–200 mg/L to reach equilibrium was 60 min.

3.4. *Point of zero charge (pH_{pzc}) studies and the effect of pH on MB adsorption*

The point of zero charge (pH_{pzc}) is an important factor that determines the linear range of pH sensitivity and then indicates the type of surface active centers and the adsorption ability of the surface [32]. Many researchers studied the point of zero charge of adsorbents that prepared from agricultural solid wastes in order to better understand of adsorption mechanism. Cationic dye adsorption is favored at $pH > pH_{pzc}$, due to the presence of functional groups such as OH^-, COO^- groups. Anionic dye adsorption

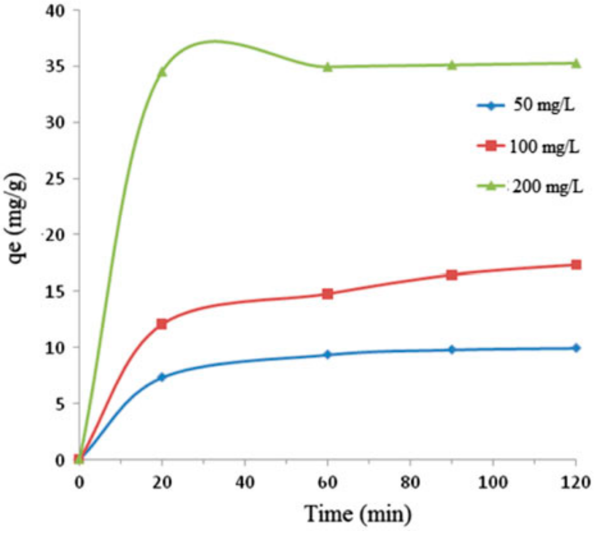

Fig. 3. Effect of contact time and initial concentration on the adsorption of MB on SMRS.

is favored at $pH < pH_{pzc}$ where the surface becomes positively charged [33,34]. The graph of pH_{final} vs. pH_{intial} is plotted as shown in Fig. 4. The intersections of the curves with the straight line are known as the end points of the pH_{pzc}, and this value is 6.8 for SMRS. Fig. 5 shows the effect of pH on the adsorption of MB. The experiments were conducted at 100 mg/L initial MB concentration, 0.10 g of SMRS dose, and 50 mL of MB solution. It was observed that pH gives a significant influence to the adsorption process. MB is cationic dye, which exists in aqueous solution in the form of positively charged ions (MB^+). As a charged species, the degree of its adsorption onto the adsorbent surface is primarily influenced by the surface charge on the adsorbent, which in turn is influenced by the solution pH. As shown in Fig. 5, the removal percentage was minimum at pH 2.0 (12%), this increased up to pH 7.0 and remained nearly constant (93%) over the initial pH ranges of 7.0–12.0. This phenomenon occurred due to the presence of excess H^+ ions in the adsorbate and the negatively charged surface adsorbent. Lower adsorption of MB at acidic pH ($pH < pH_{pzc}$) is due to the presence of excess H^+ ions competing with the cation groups on the dye for adsorption sites. At higher solution pH ($pH > pH_{pzc}$), the SMRS is possibly negatively charged and enhance the positively charged dye cations through electrostatic forces of attraction. We selected pH 7.0 for adsorption and kinetic experiments.

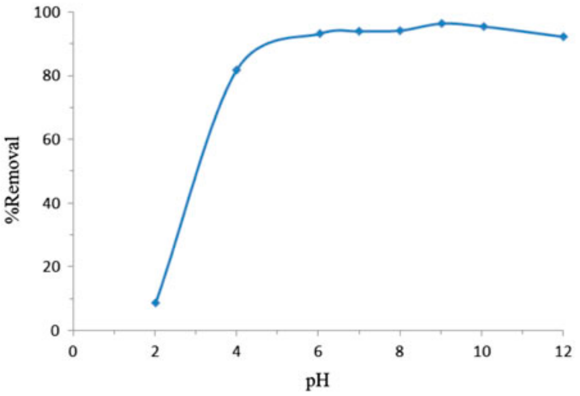

Fig. 5. Effect of solution pH on the adsorption of MB on SMRS.

3.5. Effect of adsorbent dose

Adsorbent dose is an important parameter that strongly influences the adsorption process by affecting the adsorption capacity of the adsorbent [35]. Therefore, the influence of adsorbent dose on MB adsorption by SMRS was investigated in the range of 0.05–0.6 g/100 mL of MB solution (initial concentration: 100 mg/L, pH 7.0) (Fig. 6). The adsorption efficiency increased from 85% to 96% as the adsorbent dose increased from 0.05 to 0.2 g. The increase in the percentage of dye removal with adsorbent dose could be attributed to an increase in the adsorbent surface area, augmenting the number of adsorption sites available for adsorption, as previously reported [36,37]. The decrease in sorption capacity with increasing dosage of adsorbent at constant dye concentration and volume may be attributed to saturation of adsorption sites due to the particulate interaction such as aggregation [38]. Such aggregation would lead to a decrease in total surface area of the adsorbent and an

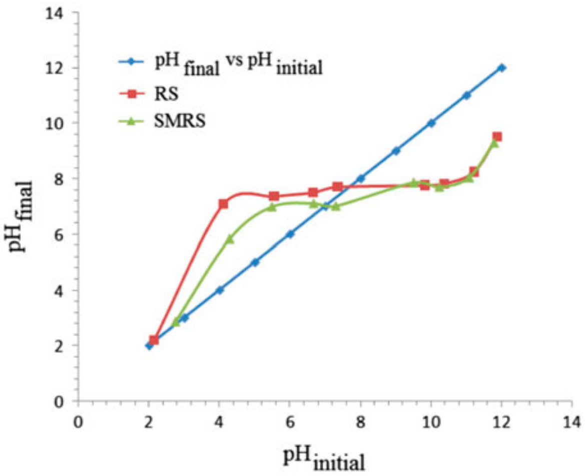

Fig. 4. Plot for determination of point of zero charge of RS and SMRS.

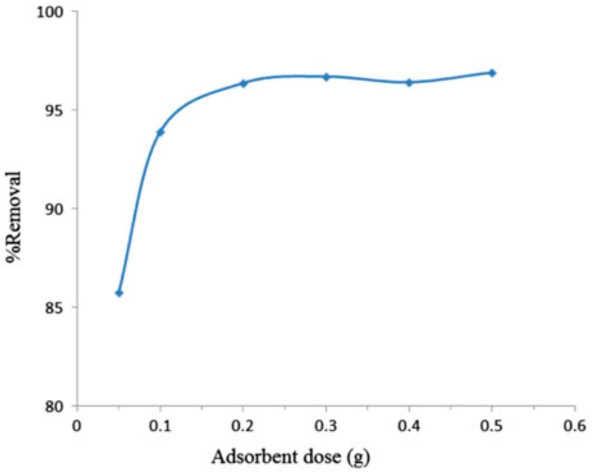

Fig. 6. Effect of adsorbent dosage on adsorption of MB on SMRS.

increase in diffusional path length [39]. Therefore, in the following experiments, the adsorbent dose was fixed at 0.2 g/100 mL.

3.6. Mechanism of MB adsorption onto SMRS

The surface modification and proposed mechanism of MB adsorption onto SMRS is shown schematically in Fig. 7. In oxides, generally, a monolayer of surfactant molecules (which is called hemimicelles) is formed with the surfactant head group facing toward the oxide surface and its hydrocarbon tail groups into solution. In the event that higher concentrations of the surfactant molecules are presented in the solution, new hydrophobic interactions between hydrocarbons tail groups will be occurred which results in the formation of discrete surface aggregates termed as admicelles. Both of these hemimicelle or admicelle regions formed on the surface of oxides are potential adsorbing locations [40]. Another possible mechanism is the hydrocarbon tail group of surfactant may interact with solid surface through hydrophobic bonding and the head group directed toward the bulk of the solution, so the surface is potential negative or positive. The mechanism was due to the adsorption of SDS onto RS surface (Fig. 7). The nonpolar portion (alkyl) of SDS may interact with RS surface through hydrophobic bonding and the polar (negative charged) head group directed toward the bulk of the solution, so the surface is potential negative. So, there is negative charge onto the surface of SMRS and the mechanism of adsorption about MB onto SMRS may include electrostatic interaction or ion exchange. Also, some of the MB molecules adsorbed onto the SMRS surface through hydrophobic interaction between MB and hydrocarbon tail of surfactant (Fig. 7).

3.7. Isotherm modeling

The fitting parameters for the measured isotherm data for MB adsorption onto SMRS in the nonlinear forms of the Langmuir and Freundlich models are presented in Fig. 8 and Table 1. By comparing the correlation coefficients R^2, it can be deduced that the experimental data are well described by the Langmuir equation compared with the Freundlich model. This suggests the monolayer coverage of the surface of SMRS by MB molecules. The high adsorption capacity in SMRS could be due to the large amount of surfactant on the surface of RS particles, which could result in increasing the amounts of negatively charged sites on the surface of RS and finally facilitates the attraction toward the positive dye molecules. Moreover, the $Q_{\max}$ decreases with an increase in temperature (from 303 to 323 K), which specifies an exothermic nature of the existing process. The Langmuir adsorption capacity, $Q_{\max}$, was found to be 296 mg/g for SMRS and 145 mg/g for RS (results not shown) at 303 K, respectively. These data showed the modification of RS by anionic surfactant increased adsorption capacity of RS.

The Freundlich equation is suitable for homogeneous and heterogeneous surfaces, indicating a multilayer adsorption [41]. The magnitude of the Freundlich constant n gives a measure of favorability of adsorption. Values of $n > 1$ represent a favorable adsorption process [36]. For the present study, the value of n also presents the same trend at all the temperatures indicating the favorable nature of adsorption of MB by SMRS.

3.8. Adsorption kinetic studies

The dynamics of the adsorption can be studied by the kinetics of adsorption in terms of the order of the rate constant [42]. The adsorption rate is an important factor for a better choice of material to be used as an adsorbent; where the adsorbent should have a large adsorption capacity and a fast adsorption rate. Most of the adsorption studies used pseudo-first-order and pseudo-second-order models to study the adsorption kinetics. For the pseudo-first-order model, the

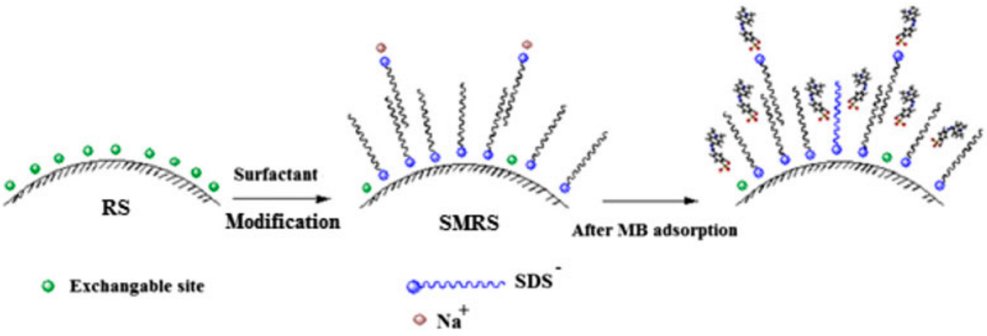

Fig. 7. Schematic illustration of proposed mechanisms for MB adsorption onto SMRS.

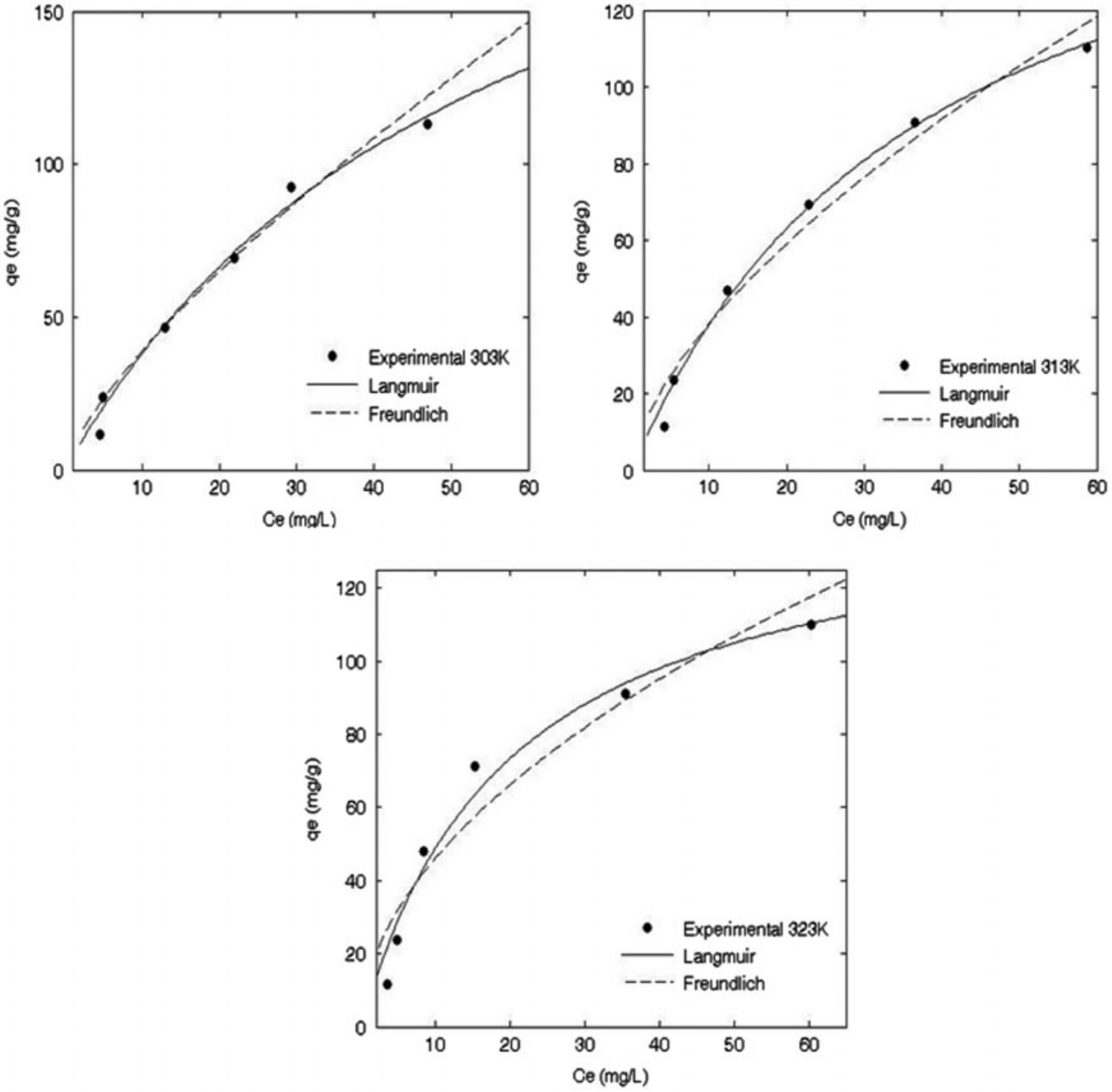

Fig. 8. Isotherm plots for MB adsorption onto SMRS at different temperatures.

adsorption rate was expected to be proportional to the first power of concentration, where the adsorption was characterized by diffusion through a boundary. The pseudo-first-order model sometimes does not fit well for the whole range of contact time when it failed theoretically to predict the amount of dye adsorbed and thus deviated from the theory. In that case, the pseudo-second-order equation used was based on the sorption capacity of the solid phase, where the pseudo-second-order model assumes that chemisorptions may be the rate-controlling step in the adsorption processes [43]. The transient behavior of the MB adsorption process was analyzed using the pseudo-first- and pseudo-second-order kinetic models. Plotting ln $(q_e - q_t)$ against t permits the calculation of

Table 1
Isotherm parameters for MB adsorption onto SMRS

Temperature (K)	303	313	323
Langmuir			
Q_{max} (mg/g)	296.74	285.72	277.78
K_L (L/mg)	0.0039	0.0044	0.0055
R^2	0.9954	0.9945	0.9934
Freundlich			
n	1.36	1.59	1.94
K_F (mg/g)(dm^3/mg)$^{1/n}$	7.08	8.96	13.96
R^2	0.9732	0.9710	0.9229

k_1 (Fig. 9(a)). The values of rate constants, k_1, evaluated from these plots with the correlation coefficients obtained are listed in Table 2. Plotting t/q against t (Fig. 9(b)) gives a straight line where k_2 can be calculated. Usually the best-fit model can be selected based on the linear regression correlation coefficient R^2 values. Generally, the kinetic adsorption is better represented by pseudo-second-order model for anionic and cationic dye adsorption. The R^2 listed (Table 2) for the pseudo-first-order kinetic model is between 0.9622 and 0.9911. The R^2 values for pseudo-second-order model were close to 1, which is higher than the R^2 values obtained for the pseudo-first-order model. Therefore, the adsorption kinetics could well be satisfactorily more favorably described by pseudo-second-order kinetic model for MB adsorption onto SMRS.

In adsorption process of dye ion on the solid surface, the dye species migrate toward the surface of the adsorbent. This type of migration proceeds till the concentration of the adsorbate species gets adsorbed onto the surface of the adsorbent. Once equilibrium is attained, the migration of the solute species from the solutions tops. Under this situation, it is possible to measure the magnitude of the distribution of the solute species between the liquid and solid phases. The magnitude of this kind of distribution is a measure of the efficiency of the chosen adsorbent in the adsorbate species. When a powdered solid adsorbent material is made in contact with a solution containing dyes, the dyes first migrate from the bulk solution to the surface of the liquid film. This surface exerts a diffusion barrier. This barrier may be very significant or less significant [44]. The involvement of a significant quantum of diffusion barrier indicates the dominant role taken up by the film diffusion in the adsorption process. Furthermore, the rate of an adsorption process is controlled either by external diffusion, internal diffusion, or by both types of diffusions. The external diffusion controls the migration of the solute species from the solution to the boundary layer of the liquid phase. However, the internal diffusion controls the transfer of the solute species from the external surface of the adsorbent to the internal surface of the pores of the adsorbent material [45]. It is now well established that, during the adsorption of dye over a porous adsorbent, the following three consecutive steps were taken place [46,47]:

(1) Transport of the ingoing adsorbate ions to external surface of the adsorbent (film diffusion).
(2) Transport of the adsorbate ions within the pores of the adsorbent except for a small amount of adsorption, which occurs on the external surface (particle diffusion).
(3) Adsorption of the ingoing adsorbate ions on the interior surface of the adsorbent.

Out of these three processes, the third process is considered to be very fast and is not the rate-limiting step in the uptake of organic compounds. The remaining two steps impart the following three possibilities:

Case 1: External transport > internal transport, where rate is governed by particle diffusion.

Case 2: External transport < internal transport, where the rate is governed by film diffusion.

Case 3: External transport ≈ internal transport, which accounts for the transport of the adsorbate ions to the boundary and may not be possible with in a significant rate, which later on gives rise to the formation of a liquid film surrounded by the adsorbent particles with a proper concentration gradient. In order to predict the actual slow step involved in the adsorption process, the kinetic data were further analyzed using the Boyd model given by Eq. (8) [48].

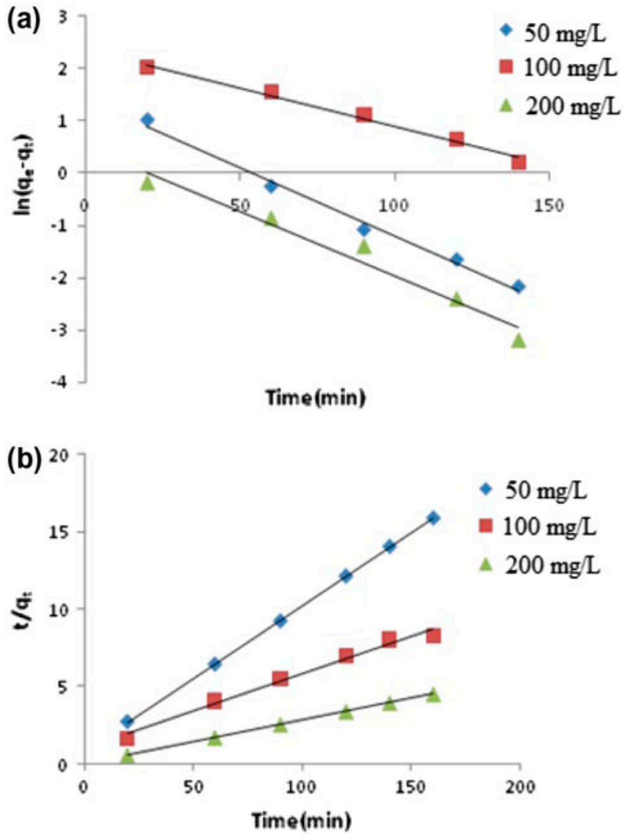

Fig. 9. Kinetic models for adsorption of MB onto SMRS.(a) pseudo-first-order and (b) pseudo-second-order rate equations.

Table 2
Kinetic parameters for the adsorption of MB onto SMRS based on the Lagergren rate equation

	Pseudo-first-order				Pseudo-second-order		
C_0 (mg/L)	q_e (mg/g)	k_1 (1/min)	R^2	q_{exp} (mg/g)	q_e (mg/g)	k_2 (g/mg min^{-1})	R^2
50	4.19	0.0263	0.9911	10.61	10.63	0.0107	0.9999
100	10.76	0.0148	0.9875	20.79	20.83	0.0232	0.9986
200	1.67	0.0248	0.9622	65.39	65.46	0.0384	0.9999

$$B_t = -0.4977 - \ln(1 - F) \tag{8}$$

where F represents the fraction of solute adsorbed at anytime, t (h), as calculated using Eq. (9):

$$F = q_t/q_e \tag{9}$$

where q_t and q_e are the amounts adsorbed after time t and after infinite time (160 min), respectively. The calculated B_t values are plotted against time t (h), as shown in Fig. 10. The plot of B_t vs. time distinguishes between the film diffusion- and particle diffusion-controlled rates of adsorption. The linear lines for all MB initial concentrations did not pass through the origin and the points were scatterd. This indicated that the adsorption of MB on the SMRS was mainly governed by external mass transport where particle diffusion was the rate-limiting step [48].

3.9. Adsorption thermodynamics

In environmental engineering practice, both energy and entropy factors must be considered in order to determine what processes will occur spontaneously [49]. Gibb's free energy change, ΔG°, is the fundamental criterion of spontaneity. Reactions occur spontaneously at a given temperature if ΔG° is a negative value. The thermodynamic parameters of ΔG°, enthalpy change, ΔH°, and entropy change, ΔS°, for the adsorption processes are calculated using the following equations [49,50]:

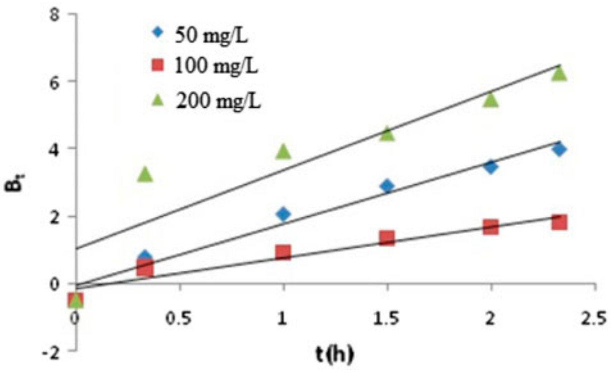

Fig. 10. Plot of B_t vs. time for different initial concentrations of MB.

$$\Delta G^{\circ} = -RT \ln K_D \tag{10}$$

K_D is given by the following equation:

$$K_D = q_e/C_e \tag{11}$$

where K_D is the distribution coefficient and

$$\ln K_D = -\Delta H^{\circ}/R(1/T) + \Delta S^{\circ}/R \tag{12}$$

where R is the universal gas constant (8.314 J/mol K) and T is the absolute temperature in K. A plot of $\ln K_D$ vs. $1/T$ was found to be linear. The values of ΔH° and ΔS° were, respectively, determined from the slope and intercept of the plot. The thermodynamic parameter, ΔG°, is shown in Table 3. ΔH° and ΔS° for the sorption process were calculated to be −0.05 kJ/mol and +3.20 J/mol K, respectively. The negative value of ΔG° confirms the feasibility of the process and the spontaneous nature of sorption with a high preference for MB to adsorb onto SMRS. The value of ΔH° was negative, indicating that the sorption reaction is exothermic. These values did not indicate strong chemisorptive bond formation between the dye molecules and the adsorbent surface. The positive value of ΔS° (Table 3) shows that the freedom of MB is not too restricted in SMRS confirming a physical adsorption, which is further confirmed by the relatively low values of ΔG°. Also, the positive ΔS° value reveals increased randomness at the interface of solid and liquid, indicating the accumulation of MB. The activation energy (E_a) was obtained from the slope of plot $\ln(1 - \theta)$ against $1/T$, where the

Table 3
Thermodynamic parameters for the adsorption of MB onto SMRS

Temperature (K)	ΔG° (kJ/mol)	ΔH° (kJ/mol)	ΔS° (J/mol K)	E_a (kJ/mol)	S^*
293	−1.644	−0.62	3.20	−0.05	0.117
313	−1.637				
323	−1.555				

surface coverage (θ) was calculated from the relation Eq. (13) [50,51]:

$$\theta = 1 - (C/C_0) \tag{13}$$

where C_0 and C are the initial and residual concentrations of MB in solution, respectively (mg/L).

In order to further support the assertion that physical adsorption is the predominant mechanism, the values of sticking probability (S^*) was estimated from the experimental data. It was calculated using a modified Arrhenius-type equation related to the surface coverage as expressed in Eq. (14) [50,52].

$$S^* = (1 - \theta)e^{-(E_a/RT)} \tag{14}$$

The parameter S^* indicates the measure of the potential of an adsorbate to remain on the adsorbent indefinitely. It can be expressed as in Table 3. The effect of temperature on the sticking probability was evaluated throughout the temperature range from 293 to 323 K by calculating the surface coverage at various temperatures. The apparent activation energy (E_a) and the sticking probability (S^*) are estimated from the plot with reasonable good fit for the MB on the SMRS. The E_a values calculated from the slope of the plot were found to be −0.05 kJ/mol. The negative values of E_a indicate that lower solution temperatures favor MB removal by adsorption onto SMRS and the adsorption process is exothermic in nature. Relatively low values of E_a suggest that MB adsorption is a diffusion-controlled process. The results as shown in Table 3 indicate that the probability of MB sticking to the SMRS surface is very high as $0 < S^* < 1$ for MB (Table 3). These values confirm that the sorption process is physisorption [52].

3.10. Desorption studies of MB

Desorption studies can help enlightening the mechanism of an adsorption process. If the dye adsorbed onto the adsorbent can be desorbed by water, it can be said that the attachment of the dye onto the adsorbent is by weak bonds. If the strong bases, such as NaOH, can desorb the dye, it can be said that the attachment of the dye onto the adsorbent is by ion exchange [53]. Hence, neutral distilled water was used in the elution of MB molecules from the SMRS followed by NaOH solution. The percentage of desorption obtained were 15 and 20% for using neutral distilled water and 0.1 N NaOH solution, respectively. The fact that the low desorption occurred with distilled water and NaOH solution suggests that adsorption of MB onto SMRS is carried out significantly by another mechanism. The mode of existence of surfactant molecules on solid surface has been investigated widely [41]. As we mentioned in section 3.6, a possible mechanism is the hydrocarbons tail group of surfactant may interact with solid surface through hydrophobic bonding and the head group directed toward the bulk of the solution, so the surface is potential negative or positive. Consequently, it can be conceived from the result of desorption by NaOH that some surfactant molecular arrange in this manner in the research. Here, the above conclusion related to ion exchange mechanism is clearly confirmed. Taking all the results that have been discussed above into account, it is proposed that enhanced hydrophobic interaction is the predominant mechanism contributing to the increased MB adsorption on the SMRS, followed by a certain amount of the cationic exchange. For better illustration of the process of adsorption, a suggested adsorption structure is shown in Fig. 7.

3.11. Cost evaluation of the adsorbent

Adsorbent cost is important to practicability. Cost of the adsorbent prepared in this work is mainly from the use of surfactant. The market price of SDS is about US $7,000 per metric ton. The cost of the prepared adsorbent is around US $680 per metric ton according to the ratio of RS to the surfactant (10:1). The market price of commercial activated carbon is about US $500–800 per metric ton. It is clear that the cost of the two adsorbent is similar. Compared with activated carbon, however, SMRS adsorbent has some advantages, such as simple preparation procedure and low energy consumption, and has good application prospect.

Table 4
Comparison of the $Q_{\max}$ based on the Langmuir isotherm of MB adsorption on various adsorbents

Adsorbent	$Q_{\max}$ (mg/g)	Refs.
Wheat straw	57.2	[54]
Modified wheat straw	266.7	[54]
Modified rice straw	208.33	[55]
Tea waste	85.5	[56]
NaOH-modified rejected tea	242.11	[57]
Modified rice straw	270	[58]
SMRS	296	This work

3.12. Comparison with other adsorbents

Table 4 shows a comparison of the maximum adsorption capacity ($Q_{\max}$ value) of SMRS with those of other low-cost adsorbents. The SMRS shows the comparable adsorption capacity for MB with respect to other low-cost adsorbents. Therefore, SMRS was suitable and promising for MB removal from aqueous solutions since it has a relatively high adsorption capacity.

4. Conclusions

The results of this investigation show that sodium dodecyle sulfate-modified RS (SMRS) has excellent adsorption capacity for the removal of MB from aqueous solutions. SEM shows that morphological feature of RS changed after modification. FTIR and SEM results suggest that the SDS have successfully coated the surface of RS. The adsorption isotherm experiment was conducted at different temperatures (303, 313, and 323 K), and it was found that the uptake of MB decreased with increasing temperature, and hence, adsorption process is exothermic in nature. The equilibrium data were analyzed by the Langmuir and Freundlich models and the Langmuir model was found to fit the equilibrium data better. The adsorption capacity was found to be 296 mg/g at 303 K. The pseudo-second-order kinetic model agrees very well with the dynamic behavior for the adsorption of MB onto surfactant-modified RS. The desorption studies implied that the hydrophobic interaction and cationic exchange models controlled simultaneously during the adsorption process, but the former is a dominant mechanism. The developed SMRS not only has demonstrated higher adsorption efficiency and fast kinetics but also have shown additional benefits like cost-effectiveness and environmental friendliness. It can be concluded to be a promising advanced adsorbent in environmental pollution cleanup.

Acknowledgments

The authors wish to acknowledge the financial support of the University of Tehran.

References

[1] M.T. Yagub, T.K. Sen, S. Afroze, H.M. Ang, Dye and its removal from aqueous solution by adsorption: A review, Adv. Colloid Interface Sci. 209 (2014) 172–184.
[2] V.K. Gupta, Suhas, Application of low-cost adsorbents for dye removal—A review, J. Environ. Manage. 90 (2009) 2313–2342.
[3] A. Bhatnagar, M. Sillanpää, Utilization of agro-industrial and municipal waste materials as potential adsorbents for water treatment—A review, Chem. Eng. J. 157 (2010) 277–296.
[4] I. Gaballah, D. Goy, E. Allain, G. Kilbertus, J. Thauront, Recovery of copper through decontamination of synthetic solutions using modified barks, Metall. Mater. Trans. B 28 (1997) 13–23.
[5] G. Crini, P.M. Badot, Application of chitosan, a natural aminopolysaccharide, for dye removal from aqueous solutions by adsorption processes using batch studies: A review of recent literature, Progress in Polym. Sci. 33 (2008) 399–447.
[6] M.A. Mohammed, A. Shitu, A. Ibrahim, Removal of methylene blue using low cost adsorbent: A review, Res. J. Chem. Sci. 4 (2014) 91–102.
[7] M.A. Oladipo, I.A. Bello, D.O. Adeoye, K.A. Abdulsalam, A.A. Giwa, Sorptive removal of dyes from aqueous solution: A review, Adv. Environ. Biol. 7 (2013) 3311–3327.
[8] M.A.Mohd Salleh, D. Khalid Mahmoud, W.A. Wan Abdul Karim, A. Idris, Cationic and anionic dye adsorption by agricultural solid wastes: A comprehensive review, Desalination 280 (2011) 1–13.
[9] A.H. Basta, V. Fierro, H. El-Saied, A. Celzard, 2-Steps KOH activation of rice straw: An efficient method for preparing high-performance activated carbons, Bioresour. Technol. 100 (2009) 3941–3947.
[10] G.M. Nabil, N.M. El-Mallah, M.E. Mahmoud, Enhanced decolorization of reactive black 5 dye by active carbon sorbent-immobilized-cationic surfactant (AC-CS), J. Ind. Eng. Chem. 20 (2014) 994–1002.
[11] M.U. Khobragade, P. Anjali, Investigation on the adsorption of Mn(II) on surfactant-modified alumina: Batch and column studies, J. Environ. Chem. Eng. 2 (2014) 2295–2305.
[12] X. Jin, B. Yu, Z. Chen, J.M. Arocena, R.W. Thring, Adsorption of Orange II dye in aqueous solution onto surfactant-coated zeolite: Characterization, kinetic and thermodynamic studies, J. Colloid Interface Sci. 435 (2014) 15–20.
[13] W. Chen, L. Pan, L. Chen, Z. Yu, Q. Wang, C. Yan, Comparison of EDTA and SDS as potential surface impregnation agents for lead adsorption by activated carbon, Appl. Surf. Sci. 309 (2014) 38–45.
[14] S. Chatterjee, D.S. Lee, M.W. Lee, S.H. Woo, Congo red adsorption from aqueous solutions by using chitosan hydrogel beads impregnated with nonionic or anionic surfactant, Bioresour. Technol. 100 (2009) 3862–3868.

[15] H. Chen, J. Zhao, J. Wu, G. Dai, Isotherm, thermodynamic, kinetics and adsorption mechanism studies of methyl orange by surfactant modified silkworm exuviae, J. Hazard. Mater. 192 (2011) 246–254.

[16] L. García-Río, P. Hervella, J.C. Mejuto, M. Parajó, Spectroscopic and kinetic investigation of the interaction between crystal violet and sodium dodecylsulfate, Chem. Phys. 335 (2007) 164–176.

[17] B. Simoncic, M. Kert, A study of anionic dye-cationic surfactant interactions in mixtures of cationic and nonionic surfactants, Dyes Pigm. 54 (2002) 221–237.

[18] K.V. Kumar, V. Ramamurthi, S. Sivanesan, Modeling the mechanism involved during the sorption of methylene blue onto fly ash, J. Colloid Interface Sci. 284 (2005) 14–21.

[19] Y. Liu, Y.J. Liu, Biosorption isotherms, kinetics and thermodynamics, Sep. Purif. Technol. 61 (2008) 229–242.

[20] S. Lagergren, About the theory of so-called adsorption of soluble substances, K. Sven. Vetenskapsakad. Handl. 24 (1898) 1–39.

[21] C.G. Rocha, D.A.M. Zaia, R.V.D. Alfaya, A.A.D. Alfaya, Use of rice straw as biosorbent for removal of Cu(II), Zn(II), Cd(II) and Hg(II) ions in industrial effluents, J. Hazard. Mater. 166 (2009) 383–388.

[22] L.C. Zheng, Z. Dang, C.F. Zhu, X.Y. Yi, H. Zhang, C. Liu, Removal of cadmium(II) from aqueous solution by corn stalk graft copolymers, Bioresour. Technol. 101 (2010) 5820–5826.

[23] G. Silva, E.C. Mattos, R.C.L. Dutra, M.F. Diniz, K. Iha, Quantitative determination of TNT and HNS by TG and FT-IR, Química Nova 31 (2008) 1431–1436.

[24] H. Chen, J. Zhao, J. Wu, G. Dai, Isotherm, thermodynamic, kinetics and adsorption mechanism studies of methyl orange by surfactant modified silkworm exuviae, J. Hazard. Mater. 192 (2011) 246–254.

[25] T.S. Anirudhan, B.F. Noeline, D.M. Manohar, Phosphate removal from wastewaters using a weak anion exchanger prepared from a lignocellulosic residue, Environ. Sci. Technol. 40 (2006) 2740–2745.

[26] K. Flogeac, E. Guillon, E. Marceau, M. Aplincourt, Speciation of chromium on a straw lignin: Adsorption isotherm, EPR, and XAS studies, New J. Chem. 27 (2003) 714–720.

[27] W. Cao, Zh Dang, X.-Q. Zhou, X.-Y. Yi, P.-X. Wu, N.-W. Zhu, G.-N. Lu, Removal of sulphate from aqueous solution using modified rice straw: Preparation, characterization and adsorption performance, Carbohydr. Polym. 85 (2011) 571–577.

[28] M. Nadeem, M. Shabbir, M.A. Abdullah, S.S. Shah, G. McKay, Sorption of cadmium from aqueous solution by surfactant-modified carbon adsorbents, Chem. Eng. J. 148 (2009) 365–370.

[29] N. Kannan, M.M. Sundaram, Kinetics and mechanism of removal of methylene blue by adsorption on various carbons—A comparative study, Dyes Pigm. 51 (2001) 25–40.

[30] Y. Bulut, H. Aydın, A kinetics and thermodynamics study of methylene blue adsorption on wheat shells, Desalination 194 (2006) 259–267.

[31] N. Nasuha, B.H. HameedAzam T. Mohd Din, Rejected tea as a potential low-cost adsorbent for the removal of methylene blue, J. Hazard. Mater. 175 (2010) 126–132.

[32] A.A. Poghossian, Determination of the pH_{pzc} of insulators surface from capacitance–voltage characteristics of MIS and EIS structures, Sens. Actuator B: Chem. 44(5) (1997) 51–553.

[33] L.R. Radovic, I.F. Silva, J.I. Ume, J.A. Menéndez, C.A. Leon, A.W. Scaroni, A.W. Scaroni, An experimental and theoretical study of the adsorption of aromatics possessing electron-with drawing and electron-donating functional groups by chemically modified activated carbons, Carbon 35 (1997) 1339–1348.

[34] D. Savova, N. Petrov, M.F. Yardim, E. Ekinci, T. Budinova, M. Razvigorova, V. Minkova, The influence of the texture and surface properties of carbon adsorbents obtained from biomass products on the adsorption of manganese ions from aqueous solution, Carbon 41 (2003) 1897–1903.

[35] S. Chakraborty, S. Chowdhury, P.D. Saha, Adsorption of Crystal Violet from aqueous solution onto NaOH-modified rice husk, Carbohydr. Polym. 86 (2011) 1533–1541.

[36] R. Ahmad, Studies on adsorption of crystal violet dye from aqueous solution onto coniferous pinus bark powder (CPBP), J. Hazard. Mater. 171 (2009) 767–773.

[37] A. Saeed, M. Sharif, M. Iqbal, Application potential of grapefruit peel as dye sorbent: Kinetics, equilibrium and mechanism of crystal violet adsorption, J. Hazard. Mater. 179 (2010) 564–572.

[38] O. Aksakal, H. Ucun, Equilibrium, kinetic and thermodynamic studies of the biosorption of textile dye (Reactive Red 195) onto *Pinus sylvestris* L, J. Hazard. Mater. 181 (2010) 666–672.

[39] G. Crini, H.N. Peindy, F. Gimbert, C. Robert, Removal of C.I. Basic Green 4 (Malachite Green) from aqueous solutions by adsorption using cyclodextrin-based adsorbent: Kinetic and equilibrium studies, Sep. Purif. Technol. 53 (2007) 97–110.

[40] A. Ariapad, M.A. Zanjanchi, M. Arvand, Efficient removal of anionic surfactant using partial template-containing MCM-41, Desalination 284 (2012) 142–149.

[41] J.C. Igwe, A.A. Abia, Maize cob and husk as adsorbent for removal Cd, Pb and Zn ions from wastewater, Phys. Sci. 2 (2003) 83–94.

[42] V. Gómez, M.S. Larrechi, M.P. Callao, Kinetic and adsorption study of acid dye removal using activated carbon, Chemosphere 69 (2007) 1151–1158.

[43] Z. Aksu, Application of biosorption for the removal of organic pollutants: A review, Process Biochem. 40 (2005) 997–1026.

[44] V.K. Gupta, A. Mittal, V. Gajbe, Adsorption and desorption studies of a water soluble dye, Quinoline Yellow, using waste materials, J. Colloid Interface Sci. 284 (2005) 89–98.

[45] V.K. Gupta, I. Ali, Suhas, D. Mohan, Equilibrium uptake and sorption dynamics for the removal of a basic dye (basic red) using low-cost adsorbents, J. Colloid Interface Sci. 265 (2003) 257–264.

[46] J. Crank, The Mathematics of Diffusion, second ed., Clarendon, Oxford, 1975.

[47] W.J. Weber, J.C. Morris, Kinetics of adsorption on carbon from solution, J. Sanit. Eng. Div. 89 (1963) 31–60.

[48] I.A.W. Tan, B.H. Hameed, Adsorption isotherms, thermodynamics and desorption studies of basic dye on activated carbon derived from oil palm empty fruit bunch, J. Appl. Sci. 10 (2010) 2565–2571.

[49] Y.S. Ho, Isotherms for the sorption of lead onto peat: Comparison of linear and non-linear methods, Pol. J. Environ. Stud. 15 (2006) 81–86.

[50] H.-J. Butt, K. Graf, M. Kappl, Physics and Chemistry of Interfaces, WILEY-VCH Verlag GmbH & Co. KGaA, Weinheim, 2003 (Chapter 9).

[51] L. Bulgariu, M. Răţoi, D. Bulgariu, M. Macoveanu, Equilibrium study of Pb(II) and Hg(II) sorption from aqueous solution by moss peat, Environ. Eng. Manage. J. 7 (2008) 511–516.

[52] M. Horsfall Jnr., A.I. Spiff, Effects of temperature on the sorption of Pb^{2+} and Cd^{2+} from aqueous solution by *Caladium bicolor* (Wild Cocoyam) biomass, Electr. J. Biotechnol. 8 (2005) 162–169.

[53] I.D. Mall, V.C. Srivastava, G.V.A. Kumar, I.M. Mishra, Characterization and utilization of mesoporous fertilizer plant waste carbon for adsorptive removal of dyes from aqueous solution, Colloids Surf., A: Physicochem. Eng. Aspects 278 (2006) 175–187.

[54] W. Zhang, H. Yan, H. Li, Z. Jiang, L. Dong, X. Kan, H. Yang, A. Li, R. Cheng, Removal of dyes from aqueous solutions by straw based adsorbents: Batch and column studies, Chem. Eng. J. 168 (2011) 1120–1127.

[55] R. Gong, Y. Jin, J. Chen, Y. Hu, J. Sun, Removal of basic dyes from aqueous solution by sorption on phosphoric acid modified rice straw, Dyes Pigm. 73 (2007) 332–337.

[56] M.T. Uddin, M.A. Islam, S. Mahmud, M. Rukanuzzaman, Adsorptive removal of methylene blue by tea waste, J. Hazard. Mater. 164 (2009) 53–60.

[57] N. Nasuha, B.H. Hameed, Adsorption of methylene blue from aqueous solution onto NaOH-modified rejected tea, Chem. Eng. J. 166 (2011) 783–786.

[58] R. Gong, K. Zhong, Y. Hu, J. Chen, G. Zhu, Thermochemical esterifying citric acid onto lignocellulose for enhancing methylene blue sorption capacity of rice straw, J. Environ. Manage. 88 (2008) 875–880.